

# Osculating orbits in Schwarzschild spacetime, with an application to extreme mass-ratio inspirals

Adam Pound and Eric Poisson

*Department of Physics, University of Guelph, Guelph, Ontario, N1G 2W1*

(Dated: December 18, 2007)

We present a method to integrate the equations of motion that govern bound, accelerated orbits in Schwarzschild spacetime. At each instant the true worldline is assumed to lie tangent to a reference geodesic, called an osculating orbit, such that the worldline evolves smoothly from one such geodesic to the next. Because a geodesic is uniquely identified by a set of constant orbital elements, the transition between osculating orbits corresponds to an evolution of the elements. In this paper we derive the evolution equations for a convenient set of orbital elements, assuming that the force acts only within the orbital plane; this is the only restriction that we impose on the formalism, and we do not assume that the force must be small. As an application of our method, we analyze the relative motion of two massive bodies, assuming that one body is much smaller than the other. Using the hybrid Schwarzschild/post-Newtonian equations of motion formulated by Kidder, Will, and Wiseman, we treat the unperturbed motion as geodesic in a Schwarzschild spacetime with a mass parameter equal to the system's total mass. The force then consists of terms that depend on the system's reduced mass. We highlight the importance of conservative terms in this force, which cause significant long-term changes in the time-dependence and phase of the relative orbit. From our results we infer some general limitations of the radiative approximation to the gravitational self-force, which uses only the dissipative terms in the force.

PACS numbers: 04.20.-q, 04.25.-g, 04.25.Nx, 04.40.-b

## I. INTRODUCTION

### A. Orbital motion in curved spacetime

Analysis of accelerated orbits in curved spacetime has historically focused on the post-Newtonian regime (see Ref. [1, 2, 3] for general reviews of the post-Newtonian formalism), since observations of orbital motion have historically been limited to weak-field systems such as the solar neighborhood and binary pulsars. However, the advent of gravitational-wave astronomy has recently necessitated an analysis of accelerated orbits in strongly-curved spacetimes. The primary examples of such orbits are extreme mass-ratio inspirals (EMRIs), in which a small compact body of mass  $m$  spirals into a supermassive black hole of mass  $M \gg m$ . Such systems promise to be excellent sources of gravitational waves for the space-based detector LISA [4]. However, accurate predictions of the emitted waveforms must account for the effect of the compact body's gravitational field on its own motion. The compact body induces a metric perturbation  $h_{\alpha\beta} = (m/M)h_{\alpha\beta}^{(1)} + \mathcal{O}(m/M)^2$ . Although the motion of the particle may be described as a geodesic in the perturbed spacetime, it is more simply treated as an accelerated worldline in the background spacetime of the unperturbed black hole. The cause of the acceleration is thus interpreted as a gravitational self-force derived from a regularized form of the field  $h_{\alpha\beta}$ . This force was first formally calculated to first order in  $m/M$  by Mino, Sasaki, and Tanaka [5], and later by Quinn and Wald [6] (see Ref. [7] for a review of recent developments). Other possible effects on the inspiraling particle, such as tidal perturbations of the central black hole, spin-orbit and

spin-spin couplings, electromagnetic interactions, and so on, can also be treated as forces acting on the body.

Although significant progress has been made in calculating these effects (see Ref. [8] for a recent review of work on EMRIs), there has been no attempt to formulate a general method of determining and characterizing the resulting motion. Implementing the first-order gravitational self-force brings a particular difficulty: The self-force on a particle is a functional of the particle's worldline, which for the first-order calculation is assumed to be a geodesic. However, the true motion is never geodesic, because of the self-force. Thus, the effect of the self-force must somehow be determined with reference to a fictitious geodesic worldline.

In this paper we present a method to integrate the equations of motion that govern accelerated motion in Schwarzschild spacetime. The method can be used for a wide class of perturbing forces; the only restrictions are that the force must keep the orbital motion bounded between a minimum and a maximum radius (the method is not suitable for the final portion of an orbit that plunges into the black hole), and that it must be acting within the plane of the orbit (although the method could be easily extended to accommodate non-planar motion). Within these restrictions the force is arbitrary, and in particular, it is not assumed to be small. Our method is a relativistic extension of the traditional method of osculating orbits, also called the method of variation of constants, in Newtonian celestial mechanics (see, e.g., Refs. [9, 10]). In this method the true worldline  $z(\lambda)$  is taken to lie tangent to a geodesic  $z_G(\lambda)$  at each value of the orbital parameter  $\lambda$ , such that the true orbit moves smoothly from one geodesic to the next. The instantaneously tangential

geodesics are referred to as osculating orbits (meaning “kissing orbits”). A geodesic is characterized by a set of constants  $I^A$ , called *orbital elements*, and the transition between osculating orbits corresponds to changes in these elements; thus, the method of osculating orbits amounts to parametrizing the true worldline as an evolving geodesic with dynamical orbital elements  $I^A(\lambda)$ .

Because it explicitly determines the position and velocity of a tangential geodesic at each instant, this method explicitly provides the information necessary to calculate the first-order gravitational self-force at each instant. Our method is therefore very well suited to the gravitational self-force problem. It also has several more general advantages. First, because the orbital elements are constant on a geodesic, the method clearly separates perturbative from non-perturbative effects. (Throughout this paper the accelerated motion of the particle is referred to as a perturbation of the geodesic motion. However, this is only to distinguish effects of acceleration from effects on a geodesic; the “perturbation” need not be small.) Second, although the orbital elements are equivalent to the set of initial conditions, they are typically chosen so as to provide direct geometric information about the orbit. If the perturbing force is very weak, then the perturbed orbit will lie very close to a geodesic for a long period of time, and changes in the orbital elements will characterize changes in the geometry of the orbit. Thus, although our method is exact, it is perhaps most useful in the context of small perturbations. Third, the orbital elements divide into two classes. The first class includes the *principal* orbital elements; these are equivalent to constants of the motion such as energy and angular momentum, and they determine the geodesic on which the particle is moving. The second class includes the *positional* orbital elements, which determine the particle’s initial position on the selected geodesic, as well as the geodesic’s spatial orientation. Generally speaking, long-term changes in the principal orbital elements are produced by dissipative terms in the perturbing force, while long-term changes in the positional elements are produced by conservative terms. Thus, this division into two classes allows one to easily separate conservative from dissipative effects of the perturbing force.

We note that this general idea of characterizing orbital evolutions by changes in the “constants” of motion has been used frequently in analyzing the effects of radiation reaction. Such analyses have typically focused on changes in the principal elements alone, neglecting the changes in positional elements, and rarely mentioning the general framework of osculating orbits. However, there have been at least two notable generalizations of the method of osculating orbits from Newtonian to relativistic mechanics: the adaptation of the method by Damour et al. to post-Newtonian binary systems [11, 12], and the formulation proposed by Mino for orbits around a Kerr black hole [13]. The formulation by Damour et al. is complete and easy to implement, but it is limited to the post-Newtonian regime. Mino’s formulation is valid

for arbitrary bound orbits in Kerr, and it was undoubtedly useful for Mino’s own purposes, but we believe that a concrete implementation of his method would not be very practical. The reason is that Mino expresses the orbits as formal Fourier expansions with unknown convergence behavior, in terms of coefficients that would be difficult to calculate in practice. It may well be that the complexity of geodesics in Kerr make a more practical parametrization impossible, but as we shall demonstrate in this paper, we can do much better for orbits in Schwarzschild spacetime. Given the limitations of previous work, we believe that it is timely to present here a practical formulation of the method of osculating orbits for bound motion in Schwarzschild spacetime. We shall first present an outline of the general method in relativistic mechanics and its connection to the traditional method in Newtonian mechanics, and we shall next specialize the method to the case of bound orbital motion in Schwarzschild spacetime.

## B. Test case: post-Newtonian binaries

We demonstrate the usefulness of our method by applying it to the relatively simple system of two compact bodies of mass  $m_1$  and  $m_2 \gg m_1$  in the post-Newtonian regime. The equations of motion for the spatial positions  $x_1^a$  and  $x_2^a$  of the bodies have been determined in harmonic coordinates to 3.5PN order (i.e. of order  $(v/c)^7$  beyond the Newtonian description) [3]. Conservative terms appear at 1PN, 2PN, and 3PN orders, and dissipative terms appear at 2.5PN and 3.5PN orders. Since the essential features of the problem are already present at 2.5PN order, we truncate the equations at that order for simplicity. These equations are valid for arbitrary mass ratios, but we focus on the extreme case in order to link our results to the self-force problem.

In order to analyze this system of equations with our method of osculating orbits, we use the hybrid equations of motion constructed by Kidder, Will, and Wiseman [14]. These equations take the schematic form

$$\frac{d^2 x^a}{dt^2} = -\frac{M}{r^2} (1 + \text{SCHW} + \mu \text{PF}). \quad (1)$$

The spatial separation vector  $x^a = x_1^a - x_2^a$  connects the two bodies, and  $M = m_1 + m_2$  and  $\mu = m_1 m_2 / M$  are respectively the total mass and reduced mass of the system. The terms in SCHW are the exact relativistic corrections to Newton’s law in a Schwarzschild spacetime of mass  $M$ , so that  $\frac{d^2 x^a}{dt^2} = -\frac{M}{r^2} (1 + \text{SCHW})$  is the exact equation for a test particle in that spacetime. The terms in  $\mu \text{PF}$  are those in the post-Newtonian expansion that depend explicitly on the reduced mass of the system (PF stands for “perturbing force”). Since the extra terms introduced within SCHW are of 3PN order and higher, the hybrid equations remain correct at 2.5PN order. However, they differ from the usual post-Newtonian equations in that they become exact in the test-mass limit  $\mu \rightarrow 0$ . This

allows us to apply our method to the post-Newtonian system by taking our osculating orbits to be geodesics in the fictitious Schwarzschild spacetime of mass  $M$ , and by deriving our perturbing force from  $\mu\text{PF}$ .

The force derived in this way is a form of the gravitational self-force, since it is produced by finite-mass effects. However, it differs nontrivially from the post-Newtonian limit of the relativistic self-force: First, the self-force is a gauge-dependent quantity which is typically calculated in the Lorenz gauge, while the hybrid equations of motion are derived within the harmonic gauge of post-Newtonian theory. Second, the Lorenz gauge ensures that the coordinates of the small body are defined in relation to the system’s center of mass [15], while here we use coordinates relative to the large mass. And third, our geodesics are in a fictitious Schwarzschild spacetime of mass  $M = m_1 + m_2$  and not in the background spacetime of the second body (of mass  $m_2$ ). The last two differences could be easily removed by formulating an alternative set of hybrid equations, but the gauge difference cannot be easily dealt with.

Given these differences, our method of osculating elements is used in this paper primarily as a practical means to integrate the hybrid equations of motion. Nevertheless, the perturbing force that we derive and the gravitational self-force share many essential features. In particular, the self-force can be expected to have conservative terms at 0PN (the Newtonian level), 1PN, and 2PN orders, etc., and dissipative terms at 2.5PN (corresponding to quadrupole radiation) and 3.5PN orders, etc.; our perturbing force has exactly the same features, except for the Newtonian correction, which is implicitly accounted for by working in terms of total and reduced masses. Thus, we can hope to draw some reasonable conclusions about the action of the gravitational self-force from our simplified analysis.

Our focus will be on detailing the limitations and ambiguities of two approximation schemes, following our analysis of the post-Newtonian electromagnetic self-force in Refs. [16, 17]. The first scheme of interest lies within the broad class of adiabatic approximations, which rest on the assumption that the accelerated orbit deviates only “slowly” from the geodesic orbit. In particular, they commonly assume that any period of the motion is much shorter than the radiation-reaction timescale of the inspiral, allowing one to eliminate irrelevant short-term oscillations and keep only secular effects. Based on this assumption, an explicit implementation of such an approximation will typically involve some type of averaging, either in the form of direct averaging of the equations of motion or via a two-timescale expansion. For clarity, we will refer to this averaging method, which is just a specific type of adiabatic approximation, as a *secular approximation*. Using the hybrid equations of motion, we show in Sec. III B that the secular approximation introduces ambiguities in the choice of (a) initial conditions and (b) the variable to be averaged over. Our results suggest that different choices can significantly affect long-term behav-

ior, and our conclusion is that while the idea of a secular approximation is attractive, the precise construction of one presents significant difficulties.

We shall also examine the (pseudo-adiabatic) *radiative approximation*, which uses the radiative (half-retarded minus half-advanced) solution to the linearized Einstein equation. As shown by Mino [18], the self-force calculated from the radiative field approximately reproduces the long-term dissipative effects of the true self-force. Largely based on this result, it was believed that the radiative approximation would produce a valid adiabatic approximation to the true evolution. This notion has led to a confusing nomenclature in the literature, in which adiabatic and radiative approximations are treated synonymously. Since the radiative approximation introduces errors beyond those of an adiabatic approximation [16, 17], we find it misleading to identify the two. We insist here that the radiative approximation is logically distinct from the class of adiabatic approximations introduced in the preceding paragraph.

Due to its simplicity, the radiative approximation has been utilized by several groups in analyzing EMRIs [19, 20]. Unfortunately, the radiative self-force neglects all conservative effects of the true self-force. In the framework of osculating orbits, this translates into neglecting long-term changes in the positional orbital elements. (Although Mino has given prescriptions for finding these long-term changes using only the radiative self-force [13, 18], his prescriptions are highly ambiguous in practice [21].) As pointed out in Ref. [20], the radiative approximation may have some utility despite this error, and in particular, it may be sufficient to generate templates for the detection of a gravitational-wave signal. But it is unlikely that it will be sufficiently accurate for reliable parameter estimation. Because of the potential usefulness of the approximation, determining its limitations is quite important. In this paper we find that neglecting conservative effects leads to long-term errors in the phase and time-dependence of the orbit; this agrees with and extends our earlier results [16, 17]. The errors in the time dependence are of particular importance, as they apply even to the evolution of the principal orbital elements.

### C. Organization of this paper

In Sec. II A we introduce the general method of osculating orbits. We then restrict our analysis in Secs. II B and II C to bound planar orbits in Schwarzschild spacetime. Section II B presents a parametrization of bound geodesics in terms of five orbital elements, and Sec. II C uses the osculation condition to find evolution equations for these orbital elements. In the second part of our paper, we apply our method to the hybrid Schwarzschild/post-Newtonian equations of motion, which are presented in Sec. III A. The results of using a secular or radiative approximation are then displayed

and discussed in Sec. III B.

## II. THE METHOD OF OSCULATING ORBITS

### A. The osculation condition

We first consider the completely general situation of a point particle moving on an arbitrary worldline  $z^\alpha(\lambda)$  parametrized by  $\lambda$ . We define the acceleration  $f^\alpha$ , or force per unit mass, acting on the particle via the equation of motion

$$\ddot{z}^\alpha + \Gamma^\alpha_{\beta\gamma} \dot{z}^\beta \dot{z}^\gamma = f^\alpha, \quad (2)$$

where an overdot indicates a derivative with respect to the proper time  $\tau$  on the worldline. The normalization condition  $\dot{z}^\alpha \dot{z}_\alpha = -1$  implies the orthogonality condition  $f^\alpha \dot{z}_\alpha = 0$ , which will be essential for later calculations. The relation between  $f^\alpha$  and the Newtonian perturbing force is discussed in Appendix A.

Using the relations  $\dot{z}^\alpha = \frac{dz^\alpha}{d\lambda} \dot{\lambda}$  and  $\ddot{z}^\alpha = \frac{d^2 z^\alpha}{d\lambda^2} \dot{\lambda}^2 + \frac{dz^\alpha}{d\lambda} \ddot{\lambda}$ , the equation of motion becomes

$$\frac{d^2 z^\alpha}{d\lambda^2} + \Gamma^\alpha_{\beta\gamma} \frac{dz^\beta}{d\lambda} \frac{dz^\gamma}{d\lambda} = f^\alpha \left( \frac{d\tau}{d\lambda} \right)^2 + \kappa(\lambda) \frac{dz^\alpha}{d\lambda}, \quad (3)$$

where  $\kappa = -\ddot{\lambda}/\dot{\lambda}^2$ . The first term on the right-hand side is due to the force acting on the particle, while the second term is present whenever  $\lambda$  is a non-affine parameter.

Our goal is to transform the equation of motion (3) into evolution equations for a set of orbital elements  $I^A$ . That is, we seek a transformation  $\{z^\alpha, \dot{z}^\alpha\} \rightarrow I^A$ . Letting  $z_G^\alpha(I^A, \lambda)$  be a geodesic with orbital elements  $I^A$ , the *osculation condition* states the following:

$$z^\alpha(\lambda) = z_G^\alpha(I^A(\lambda), \lambda), \quad (4)$$

$$\frac{dz^\alpha}{d\lambda}(\lambda) = \frac{\partial z_G^\alpha}{\partial \lambda}(I^A(\lambda), \lambda), \quad (5)$$

where the partial derivative in the second equation holds  $I^A$  fixed. These two equations assert that at each value of  $\lambda$  we can find a set of orbital elements  $I^A(\lambda)$  such that the geodesic with those elements has the same position and velocity as the accelerated orbit. We can freely make this assertion because the number of orbital elements is equal to the number of degrees of freedom on the orbit.

As a consequence of the osculation condition, all relations that are obtained using only algebraic manipulations of coordinates and velocities on a geodesic are also valid on the true orbit. However, it is important to note that  $\kappa$  is altered by the acceleration of the worldline, because it involves second derivatives. Hence, an expression for  $\kappa(\lambda)$  that is valid on an osculating geodesic will not be valid on the tangential accelerated orbit. Nevertheless,  $\ddot{\lambda} = 0$  for an affine parameter  $\lambda$  on both orbits, so affine parameters remain affine.

Now, combining the osculation condition with the equations of motion generates evolution equations for  $I^A$ .

From Eq. (4) we have that  $\frac{dz^\alpha}{d\lambda} = \frac{dz_G^\alpha}{d\lambda}$ , which implies  $\frac{dz^\alpha}{d\lambda} = \frac{\partial z_G^\alpha}{\partial \lambda} + \frac{\partial z_G^\alpha}{\partial I^A} \frac{dI^A}{d\lambda}$ , where the index  $A$  is summed over. Comparing this result with Eq. (5), we find

$$\frac{\partial z_G^\alpha}{\partial I^A} \frac{dI^A}{d\lambda} = 0. \quad (6)$$

Furthermore,  $z_G^\alpha$  satisfies the geodesic equation

$$\frac{\partial^2 z_G^\alpha}{\partial \lambda^2} + \Gamma^\alpha_{\beta\gamma} \frac{\partial z_G^\beta}{\partial \lambda} \frac{\partial z_G^\gamma}{\partial \lambda} = \kappa_G(\lambda) \frac{\partial z_G^\alpha}{\partial \lambda}, \quad (7)$$

where  $\kappa_G(\lambda)$  is the measure of non-affinity of  $\lambda$  on the geodesic. Subtracting this geodesic equation from the equation of motion (3) and using Eq. (5) to remove the Christoffel terms, we obtain

$$\frac{d^2 z^\alpha}{d\lambda^2} = \frac{\partial^2 z_G^\alpha}{\partial \lambda^2} + f^\alpha \left( \frac{d\tau}{d\lambda} \right)^2 + [\kappa(\lambda) - \kappa_G(\lambda)] \frac{\partial z_G^\alpha}{\partial \lambda}. \quad (8)$$

But differentiating Eq. (5) yields  $\frac{d^2 z^\alpha}{d\lambda^2} = \frac{\partial^2 z_G^\alpha}{\partial \lambda^2} + \left( \frac{\partial}{\partial I^A} \frac{\partial z_G^\alpha}{\partial \lambda} \right) \frac{dI^A}{d\lambda}$ . Comparing these results, we find

$$\left( \frac{\partial}{\partial I^A} \frac{\partial z_G^\alpha}{\partial \lambda} \right) \frac{dI^A}{d\lambda} = f^\alpha \left( \frac{d\tau}{d\lambda} \right)^2 + [\kappa(\lambda) - \kappa_G(\lambda)] \frac{\partial z_G^\alpha}{\partial \lambda}. \quad (9)$$

Equations (6) and (9) form a closed system of first-order differential equations for the orbital elements  $I^A$ . Two sources of change in the orbital elements are apparent: a direct source due to the perturbing force  $f^\alpha$ , and an indirect source due to the change in the affinity of the parametrization of the accelerated orbit. Determining this second effect in practice may be somewhat difficult. However, if we use the affine parameter  $\lambda = \tau$  then the equations simplify to

$$\frac{\partial z_G^\alpha}{\partial I^A} \dot{I}^A = 0, \quad (10)$$

$$\frac{\partial \dot{z}_G^\alpha}{\partial I^A} \dot{I}^A = f^\alpha. \quad (11)$$

These equations can be easily inverted to solve for the derivatives  $\dot{I}^A$ , which is done in Sec. II C. If a non-affine parameter  $\lambda$  is required in a specific application, one may easily find  $\frac{dI^A}{d\lambda}$  by multiplying the above equations by  $\frac{d\tau}{d\lambda}$ , which will also be done in Sec. II C.

### B. Geodesics in Schwarzschild spacetime

We now focus on the specific case of bound orbits in Schwarzschild spacetime. The osculating orbits in this case are bound geodesics, for which we use the parametrization presented in the text by Chandrasekhar [22] and described in detail in Ref. [23]. This

parametrization is given in Schwarzschild coordinates and can be easily derived as follows.

Because of the spherical symmetry of the Schwarzschild spacetime, we can freely set  $\theta = \pi/2$ . The geodesic equations in a Schwarzschild spacetime with mass parameter  $M$  can be easily solved for the remaining coordinates to find

$$\dot{t} = E/F, \quad (12)$$

$$\dot{r}^2 = E^2 - U_{\text{eff}}, \quad (13)$$

$$\dot{\phi} = \frac{L}{r^2}, \quad (14)$$

where  $F = 1 - 2M/r$ ,  $E$  and  $L$  are constants equal to energy and angular momentum per unit mass, respectively, the effective potential is  $U_{\text{eff}} = F(1 + L/r^2)$ , and an overdot represents a derivative with respect to the proper time  $\tau$  on the orbit.

We are interested in bound orbits that oscillate between a minimal radius  $r_1$  and a maximal radius  $r_2$ , respectively referred to as periapsis and apoapsis. Adapting the tradition of celestial mechanics, we define the (dimensionless) semi-latus rectum  $p$  and the eccentricity  $e$  such that the turning points are given by

$$r_1 = \frac{pM}{1+e}, \quad (15)$$

$$r_2 = \frac{pM}{1-e}, \quad (16)$$

where  $0 \leq e < 1$ . These two constants describe the geometry of the orbit, just as in Keplerian orbits:  $p$  is a measure of the radial extension of the orbit, while  $e$  is a measure of its deviation from circularity. These constants can be related to  $E$  and  $L$  by letting  $\dot{r} = 0$  in Eq. (13), which leads to

$$E^2 = \frac{(p-2-2e)(p-2+2e)}{p(p-3-e^2)}, \quad (17)$$

$$L^2 = \frac{p^2 M^2}{p-3-e^2}. \quad (18)$$

Continuing to exploit the analogy with Keplerian orbits, we introduce a parameter  $\chi$  that runs from 0 to  $2\pi$  over one radial cycle, such that  $r(\chi)$  takes the elliptical form

$$r(\chi) = \frac{pM}{1+e \cos(\chi-w)}, \quad (19)$$

where  $w$  is the value of  $\chi$  at periapsis, referred to as the argument of periapsis. The radial component of the velocity is hence

$$r'(\chi) = \frac{pMe \sin(\chi-w)}{[1+e \cos(\chi-w)]^2}, \quad (20)$$

where a prime henceforth indicates a derivative with respect to  $\chi$ .

From these results we can relate the parameter  $\chi$  to the proper time  $\tau$  using  $\frac{d\tau}{d\chi} = \frac{r'}{F}$ , which yields

$$\frac{d\tau}{d\chi} = \frac{p^{3/2} M (p-3-e^2)^{1/2}}{(p-6-2e \cos v)^{1/2} (1+e \cos v)^2}, \quad (21)$$

where we have introduced the variable

$$v \equiv \chi - w \quad (22)$$

for brevity. Along with Eqs. (12), (14), (17), and (18), this leads to the following parametrizations for  $t(\chi)$  and  $\phi(\chi)$ :

$$\phi(\chi) = \Phi + \int_w^\chi \phi'(\tilde{\chi}) d\tilde{\chi}, \quad (23)$$

$$\phi'(\chi) = \sqrt{\frac{p}{p-6-2e \cos v}}, \quad (24)$$

$$t(\chi) = T + \int_w^\chi t'(\tilde{\chi}) d\tilde{\chi}, \quad (25)$$

$$t'(\chi) = \frac{p^2 M}{(p-2-2e \cos v)(1+e \cos v)^2} \times \sqrt{\frac{(p-2-2e)(p-2+2e)}{p-6-2e \cos v}}, \quad (26)$$

where we have defined the constants  $T$  and  $\Phi$  as the values of  $t$  and  $\phi$  at periapsis, respectively.

Our parametrization of bound geodesics consists of Eqs. (19), (20), and (23)–(26). We see that a geodesic is uniquely specified by the orbital elements  $I^A = \{p, e, w, T, \Phi\}$ . The principal elements  $p$  and  $e$  determine the spatial shape of the orbit and are equivalent to specifications of energy and angular momentum; they determine the choice of geodesic. The positional elements  $w$ ,  $T$ , and  $\Phi$  determine the spatial orientation and time-dependence of the orbit; they determine the starting point of the particle on the selected geodesic. All together, the specification of the orbital elements is equivalent to the specification of initial values for the position and velocity of the particle. We need three initial positions for a planar orbit, and we need two initial velocities (three minus one, by virtue of the normalization condition on the velocity vector); this counting matches the number of orbital elements.

We note that our choice of orbital elements is closely related to Mino's in Ref. [13]. When the orbital motion is restricted to the equatorial plane of a Kerr black hole, Mino uses the principal elements  $E$  and  $L$  and positional elements that are identical to our  $w$ ,  $T$ , and  $\Phi$ . To use  $(p, e)$  instead of  $(E, L)$  is mostly a matter of taste; we believe that the set  $(p, e)$  is more useful than  $(E, L)$  because it gives a simpler parametrization, and because  $p$  and  $e$  are geometrically more informative. In the following subsection we will deviate more strongly from Mino's parametrization: for reasons that will be explained, we shall avoid directly evolving the elements  $T$  and  $\Phi$ .

All the equations presented in this section remain valid for a perturbed orbit, with the exception of Eqs. (15) and (16), which lose their meaning. The alteration that we shall make to account for the perturbation is that in each equation, the orbital elements will become functions of  $\chi$ .

### C. Evolution equations

If we restrict the perturbing force to lie in the plane of the orbit, and assume that the orbit remains bound, then the geodesics described in the last section form a sufficient set of osculating orbits. Using our parametrization of these geodesics, along with the results of our general analysis in Sec. II A, we can now find evolution equations for the orbital elements. Multiplying both sides of Eq. (10) by  $\frac{d\tau}{d\chi}$ , we find

$$\frac{\partial r}{\partial p}p' + \frac{\partial r}{\partial e}e' + \frac{\partial r}{\partial w}w' = 0, \quad (27)$$

$$\frac{\partial t}{\partial p}p' + \frac{\partial t}{\partial e}e' + \frac{\partial t}{\partial w}w' + T' = 0, \quad (28)$$

$$\frac{\partial \phi}{\partial p}p' + \frac{\partial \phi}{\partial e}e' + \frac{\partial \phi}{\partial w}w' + \Phi' = 0. \quad (29)$$

Similarly, from Eq. (11) we find

$$\frac{\partial \dot{t}}{\partial p}p' + \frac{\partial \dot{t}}{\partial e}e' + \frac{\partial \dot{t}}{\partial w}w' = f^t \tau', \quad (30)$$

$$\frac{\partial \dot{r}}{\partial p}p' + \frac{\partial \dot{r}}{\partial e}e' + \frac{\partial \dot{r}}{\partial w}w' = f^r \tau', \quad (31)$$

$$\frac{\partial \dot{\phi}}{\partial p}p' + \frac{\partial \dot{\phi}}{\partial e}e' + \frac{\partial \dot{\phi}}{\partial w}w' = f^\phi \tau'. \quad (32)$$

The orthogonality condition  $f^\alpha \dot{z}_\alpha = 0$  allows us to remove one component of Eq. (11) from the set of equations; we use this freedom to remove Eq. (30). The remaining equations decouple into a closed system of ordinary differential equations for  $p$ ,  $e$ , and  $w$  and two auxiliary equations for  $T$  and  $\Phi$ . We shall find that the evolution equations for  $p$ ,  $e$ , and  $w$  are simple. The equations for  $T$  and  $\Phi$ , however, are not: Factors such as  $\frac{\partial \dot{t}}{\partial p}$  in Eqs. (28) and (29) introduce elliptic integrals of the form  $\int_w^\chi \frac{\partial t'}{\partial p}(\tilde{\chi})d\tilde{\chi}$  into the expressions for  $T'$  and  $\Phi'$ . These

integrals would have to be evaluated at each time-step in a numerical evolution, and they would create an excessive computational cost. Additionally, the integrals generally grow linearly with  $\chi$ , and this produces terms in  $T(\chi)$  and  $\Phi(\chi)$  that grow quadratically with  $\chi$ , as well as terms that oscillate with a linearly increasing amplitude. Such terms greatly confuse both numerical and analytical descriptions, and they are largely an artefact of our parametrization. (This statement applies also to Mino's parametrization [13].) We note that similar (though less severe) difficulties arise also in the method of osculating orbits in Newtonian celestial mechanics; refer for example to the discussion on pp. 248–250 in the text by Beutler [10]. In the Newtonian context, alternative orbital elements are typically selected so as to overcome these problems. With no obvious choice of alternative elements in the relativistic context, we opt instead to directly evolve the coordinates  $t$  and  $\phi$  rather than the elements  $T$  and  $\Phi$ .

Our phase space thus consists of  $\{p, e, w, t, \phi\}$ . This choice of phase space does not allow an easy separation of perturbative from geodesic effects in the evolutions of  $t$  and  $\phi$ , nor does it allow a clean separation of conservative from dissipative effects. But it is overwhelmingly more convenient than the alternative choice  $\{p, e, w, T, \Phi\}$ . If  $T$  and  $\Phi$  are required in an application, they may be found as, e.g.,  $T = t - \int_w^\chi t'(\tilde{\chi})d\tilde{\chi}$ . This may be necessary if initial conditions are required on an osculating orbit, or if one wishes to fully isolate perturbative effects.

Solving for  $w'$  from Eq. (27), and noting that  $\frac{\partial r}{\partial w} = -r'$ , we find

$$w' = \frac{1}{r'} \left( \frac{\partial r}{\partial p}p' + \frac{\partial r}{\partial e}e' \right). \quad (33)$$

Substituting this into Eqs. (30) and (32), we can solve for  $p'$  and  $e'$  to find

$$p' = \frac{\mathcal{L}_e(\phi)f^r - \mathcal{L}_e(r)f^\phi}{\mathcal{L}_e(\phi)\mathcal{L}_p(r) - \mathcal{L}_e(r)\mathcal{L}_p(\phi)}\tau', \quad (34)$$

$$e' = \frac{\mathcal{L}_p(r)f^\phi - \mathcal{L}_p(\phi)f^r}{\mathcal{L}_e(\phi)\mathcal{L}_p(r) - \mathcal{L}_e(r)\mathcal{L}_p(\phi)}\tau', \quad (35)$$

where  $\mathcal{L}_a(x) \equiv \frac{\partial \dot{x}}{\partial a} + \frac{1}{r'} \frac{\partial r}{\partial a} \frac{\partial \dot{x}}{\partial w}$ . Explicitly, the results are

$$p' = \frac{2p^{7/2}M^2(p-3-e^2)(p-6-2e\cos v)^{1/2}(p-3-e^2\cos^2 v)}{(p-6+2e)(p-6-2e)(1+e\cos v)^4}f^\phi - \frac{2p^3Me(p-3-e^2)\sin v}{(p-6+2e)(p-6-2e)(1+e\cos v)^2}f^r, \quad (36)$$

$$e' = \frac{p^{5/2}M^2(p-3-e^2)\{(p-6-2e^2)[(p-6-2e\cos v)e\cos v+2(p-3)]\cos v+e(p^2-10p+12+4e^2)\}}{(p-6+2e)(p-6-2e)(p-6-2e\cos v)^{1/2}(1+e\cos v)^4}f^\phi + \frac{p^2M(p-3-e^2)(p-6-2e^2)\sin v}{(p-6+2e)(p-6-2e)(1+e\cos v)^2}f^r, \quad (37)$$

$$w' = \frac{p^{5/2}M^2(p-3-e^2)\{(p-6)[(p-6-2e\cos v)e\cos v+2(p-3)]-4e^3\cos v\}\sin v}{e(p-6+2e)(p-6-2e)(p-6-2e\cos v)^{1/2}(1+e\cos v)^4}f^\phi - \frac{p^2M(p-3-e^2)[(p-6)\cos v+2e]}{e(p-6+2e)(p-6-2e)(1+e\cos v)^2}f^r. \quad (38)$$

These equations could be rewritten in any number of ways, in terms of alternative linear combinations of  $f^t$ ,  $f^r$ , and  $f^\phi$ , by using the orthogonality relation  $f_\alpha \dot{z}^\alpha = 0$ , which has the explicit form

$$Ft'f^t - F^{-1}r'f^r - r^2\phi'f^\phi = 0. \quad (39)$$

The result of such a rearrangement might in fact be simpler, but it may also be ill-behaved from a numerical point of view. One such alternative combination is given in Appendix B.

Our first formulation of the method of osculating orbits is complete. We have first-order evolution equations for each one of the dynamical variables in the set  $\{p, e, w, t, \phi\}$ ; the equations for  $t$  and  $\phi$  were obtained in the preceding subsection, and for convenience they are reproduced here:

$$t' = \frac{p^2M}{(p-2-2e\cos v)(1+e\cos v)^2} \times \sqrt{\frac{(p-2-2e)(p-2+2e)}{p-6-2e\cos v}}, \quad (40)$$

$$\phi' = \sqrt{\frac{p}{p-6-2e\cos v}}. \quad (41)$$

Equations (36), (37), and (38) form a complete set of equations for  $p(\chi)$ ,  $e(\chi)$ , and  $w(\chi)$ ; once these functions are known,  $t(\chi)$  and  $\phi(\chi)$  can be obtained from the remaining two equations. We recall that  $v = \chi - w(\chi)$ .

One may note that  $w'$  diverges as  $e \rightarrow 0$ . This corresponds to the fact that  $w$  loses its geometric meaning for circular orbits. To overcome this difficulty we can again follow celestial mechanics and define alternative orbital elements  $\alpha = e \sin w$  and  $\beta = e \cos w$ . The radial coordinate in terms of these elements is

$$r = \frac{pM}{1 + \Psi + \Omega}, \quad (42)$$

where  $\Psi = \alpha \sin \chi$  and  $\Omega = \beta \cos \chi$  are introduced for the sake of brevity in later expressions. While  $\alpha$  and  $\beta$  do not possess a clear geometric meaning, which limits their usefulness for generic orbits, they do allow one to analyze small-eccentricity or quasi-circular orbits. Their evolution equations can be easily calculated as  $\alpha' = e' \sin w + ew' \cos w$  and  $\beta' = e' \cos w - ew' \sin w$ . Using the identities  $e \cos v = \alpha \sin \chi + \beta \cos \chi$  and  $e \sin v = \beta \sin \chi - \alpha \cos \chi$  to simplify the results, we find

$$\beta' = \frac{p^{5/2}M^2(p-3-\alpha^2-\beta^2)f^\phi}{\sqrt{p-6-2(\Psi+\Omega)}((p-6)^2-4(\alpha^2+\beta^2))(1+\Psi+\Omega)^4} \times \left\{ -4\alpha \left[ \alpha\beta \cos 2\chi + \frac{1}{2}(\alpha^2-\beta^2) \sin 2\chi \right] \right. \\ \left. + [2(p-3) + (p-6)(\Psi+\Omega) - 2(\Psi+\Omega)^2] [(p-6) \cos \chi - 2\beta(\Psi+\Omega)] + \beta [p^2 - 10p + 12 + 4(\alpha^2+\beta^2)] \right\} \\ + \frac{p^2M(p-3-\alpha^2-\beta^2) [(p-6-2\beta^2) \sin \chi + 2\alpha(1+\Omega)] f^r}{((p-6)^2-4(\alpha^2+\beta^2))(1+\Psi+\Omega)^2}, \quad (43)$$

$$\alpha' = \frac{p^{5/2}M^2(p-3-\alpha^2-\beta^2)f^\phi}{\sqrt{p-6-2(\Psi+\Omega)}((p-6)^2-4(\alpha^2+\beta^2))(1+\Psi+\Omega)^4} \times \left\{ 4\beta \left[ \alpha\beta \cos 2\chi + \frac{1}{2}(\alpha^2-\beta^2) \sin 2\chi \right] \right. \\ \left. + [2(p-3) + (p-6)(\Psi+\Omega) - 2(\Psi+\Omega)^2] [(p-6) \sin \chi - 2\alpha(\Psi+\Omega)] + \alpha [p^2 - 10p + 12 + 4(\alpha^2+\beta^2)] \right\} \\ - \frac{p^2M(p-3-\alpha^2-\beta^2) [(p-6-2\alpha^2) \cos \chi + 2\beta(1+\Psi)] f^r}{((p-6)^2-4(\alpha^2+\beta^2))(1+\Psi+\Omega)^2}. \quad (44)$$

To evolve our full system we must also express  $p'$ ,  $t'$ , and  $\phi'$  in terms of  $\alpha$  and  $\beta$ :

$$p' = \frac{2p^{7/2}M^2\sqrt{p-6-2(\Psi+\Omega)}(p-3-\alpha^2-\beta^2)(p-3-(\Psi+\Omega)^2)f^\phi}{[(p-6)^2-4(\alpha^2+\beta^2)](1+\Psi+\Omega)^4} \\ - \frac{2p^3M(p-3-\alpha^2-\beta^2)(\beta \sin \chi - \alpha \cos \chi)f^r}{[(p-6)^2-4(\alpha^2+\beta^2)](1+\Psi+\Omega)^2}, \quad (45)$$

$$t'(\chi) = \frac{p^2M\sqrt{(p-2)^2-4(\alpha^2+\beta^2)}}{(p-2-2(\Psi+\Omega))\sqrt{p-6-2(\Psi+\Omega)}(1+\Psi+\Omega)^2}, \quad (46)$$

$$\phi'(\chi) = \sqrt{\frac{p}{p-6-2(\Psi+\Omega)}}. \quad (47)$$

This is our second formulation of the method of osculating orbits. The first formulation involves shorter equations, but it becomes ill-behaved when  $e$  is small. The second formulation is well behaved, but it involves longer equations.

### III. POST-NEWTONIAN BINARIES

#### A. Hybrid equations of motion

We now move on to a concrete application of our method by considering the post-Newtonian binary system introduced in Sec. IB. This system consists of two gravitationally-bound bodies of mass  $m_1$  and  $m_2$ , with equations of motion derived to 2.5PN order in a post-Newtonian expansion; because we are interested in self-force effects, we take the ratio  $m_1/m_2$  to be small, and we neglect the spin of the bodies. In this section we explain how such a system can be analyzed with our method of osculating orbits.

Our analysis is based upon the hybrid equations of motion presented in Ref. [14]. These equations begin

with the 2.5PN equations of motion for each one of the two bodies. Within the center-of-mass frame the relative motion of the two bodies is governed by the closed system of equations [24]

$$\frac{d^2 x_h^a}{dt^2} = -\frac{M}{r_h^2} \left( A \frac{x_h^a}{r_h} + B \frac{dx_h^a}{dt} \right), \quad (48)$$

where  $x_h^a \equiv x_1^a - x_2^a$  is a Cartesian spatial vector from  $m_2$  to  $m_1$  in harmonic coordinates,  $r_h^2 = \delta_{ab}x_h^a x_h^b$  is the square of the vector's Euclidean magnitude,  $t$  is a harmonic time coordinate, and  $M = m_1 + m_2$  is the total mass of the system. The functions  $A$  and  $B$  depend only on the total mass  $M$ , the reduced mass  $\mu = m_1 m_2 / M$ , and the relative coordinates and velocities. They can be written as  $A = A_M + \epsilon \tilde{A}$  and  $B = B_M + \epsilon \tilde{B}$ , where  $\epsilon = \mu/M$  and terms with a subscript  $M$  are independent of  $\mu$ . The  $\mu$ -dependent terms are quadratic in  $\epsilon$ , and they can be further decomposed into post-Newtonian orders as  $\tilde{A} = \tilde{A}_1 + \tilde{A}_2 + \tilde{A}_{2.5}$  and  $\tilde{B} = \tilde{B}_1 + \tilde{B}_2 + \tilde{B}_{2.5}$ .



Explicitly, these have the form

$$A_M = 1 - 4\frac{M}{r_h} + v^2 + 9\left(\frac{M}{r_h}\right)^2 - 2\frac{M}{r_h}\left(\frac{dr_h}{dt}\right)^2, \quad (49)$$

$$\epsilon\tilde{A}_1 = -\epsilon\left[2\frac{M}{r_h} - 3v^2 + \frac{3}{2}\left(\frac{dr_h}{dt}\right)^2\right], \quad (50)$$

$$\begin{aligned} \epsilon\tilde{A}_2 = \epsilon\left[ & \frac{87}{4}\left(\frac{M}{r_h}\right)^2 + (3-4\epsilon)v^4 - \frac{1}{2}(13-4\epsilon)\frac{M}{r_h}v^2 \right. \\ & - \frac{3}{2}(3-4\epsilon)v^2\left(\frac{dr_h}{dt}\right)^2 + \frac{15}{8}(1-3\epsilon)\left(\frac{dr_h}{dt}\right)^4 \\ & \left. - (25+2\epsilon)\frac{M}{r_h}\left(\frac{dr_h}{dt}\right)^2\right], \quad (51) \end{aligned}$$

$$\epsilon\tilde{A}_{2.5} = -\frac{8}{5}\epsilon\frac{M}{r_h}\frac{dr_h}{dt}\left[3v^2 + \frac{17}{3}\frac{M}{r_h}\right], \quad (52)$$

$$B_M = -\frac{dr_h}{dt}\left(4 - 2\frac{M}{r_h}\right), \quad (53)$$

$$\epsilon\tilde{B}_1 = 2\epsilon\frac{dr_h}{dt}, \quad (54)$$

$$\begin{aligned} \epsilon\tilde{B}_2 = -\frac{1}{2}\epsilon\frac{dr_h}{dt}\left[ & (15+4\epsilon)v^2 - (41+8\epsilon)\frac{M}{r_h} \right. \\ & \left. - 3(3+2\epsilon)\left(\frac{dr_h}{dt}\right)^2\right], \quad (55) \end{aligned}$$

$$\epsilon\tilde{B}_{2.5} = \frac{8}{5}\epsilon\frac{M}{r_h}\left[v^2 + 3\frac{M}{r_h}\right], \quad (56)$$

where  $v^2 \equiv \delta_{ab}\frac{dx_h^a}{dt}\frac{dx_h^b}{dt}$  is the square of the velocity vector in harmonic coordinates.

The hybrid equations are inspired by the fact that when  $\epsilon = 0$ , Eq. (48) becomes identical to a 2PN expansion of the geodesic equation in a Schwarzschild spacetime with mass parameter  $M$ . Building on this fact, Kidder, Will, and Wiseman [14] replaced  $A_M$  and  $B_M$  with their exact geodesic expressions  $A_S$  and  $B_S$  in the fictitious Schwarzschild spacetime. In other words, the hybrid equations of motion are given by Eq. (48) after substituting  $A = A_S + \epsilon\tilde{A}$  and  $B = B_S + \epsilon\tilde{B}$ , where

$$\begin{aligned} A_S = & \frac{1 - M/r_h}{(1 + M/r_h)^3} \\ & - \frac{2 - M/r_h}{1 - M^2/r_h^2}\frac{M}{r_h}\left(\frac{dr_h}{dt}\right)^2 + v^2, \quad (57) \end{aligned}$$

$$B_S = -\frac{4 - 2M/r_h}{1 - M^2/r_h^2}\frac{dr_h}{dt}. \quad (58)$$

The resulting equations are accurate to 2.5PN order, but in the test-mass limit  $m_1 \rightarrow 0$  they exactly describe the orbit of the test mass in the Schwarzschild spacetime of the other body. These equations form an ideal test case for our method of osculating orbits because, besides their relative simplicity, they explicitly split into

geodesic terms and perturbation terms. This allows us to construct osculating orbits as geodesics in the fictitious Schwarzschild spacetime of mass  $M$ . We can then easily derive the perturbing force from the terms  $\tilde{A}$  and  $\tilde{B}$ .

The first step in this process is to write the equations of motion in plane polar coordinates  $(r_h, \phi)$ , which are defined by  $x_h^1 = r_h \cos(\phi)$  and  $x_h^2 = r_h \sin(\phi)$ . In terms of these coordinates, Eq. (48) becomes

$$\frac{d^2 r_h}{dt^2} = -\frac{M}{r_h^2}\left(A + B\frac{dr_h}{dt}\right) + r_h\left(\frac{d\phi}{dt}\right)^2, \quad (59)$$

$$\frac{d^2 \phi}{dt^2} = -\frac{M}{r_h^2}B\frac{d\phi}{dt} - \frac{2}{r_h}\frac{dr_h}{dt}\frac{d\phi}{dt}. \quad (60)$$

The harmonic coordinates used here are related to Schwarzschild coordinates by the simple transformation  $r_h = r - M$ . Since  $M$  is constant, the subscript  $h$  can be safely dropped within derivatives. Expressing  $r_h$  in terms of  $r$ , the above equations are transformed into Schwarzschild coordinates.

We derive  $f^\alpha$  from these equations as follows. From Eq. (3) we have

$$f^\alpha = \dot{t}^2\left(\frac{d^2 z^\alpha}{dt^2} + \Gamma^\alpha_{\beta\gamma}\frac{dz^\beta}{dt}\frac{dz^\gamma}{dt} - \kappa(t)\frac{dz^\alpha}{dt}\right). \quad (61)$$

Although we could calculate  $\kappa(t)$  directly from its definition, the result would be unwieldy. We instead use the equation of motion for  $t$ ,

$$\frac{d^2 t}{dt^2} + \Gamma^t_{\beta\gamma}\frac{dz^\beta}{dt}\frac{dz^\gamma}{dt} = f^t \dot{t}^{-2} + \kappa\frac{dt}{dt}, \quad (62)$$

to replace  $\kappa$  with

$$\kappa = \Gamma^t_{\beta\gamma}\frac{dz^\beta}{dt}\frac{dz^\gamma}{dt} - f^t \dot{t}^{-2}. \quad (63)$$

Substituting this expression for  $\kappa$  into Eq. (61), we find

$$f^\alpha = \dot{t}^2 a_p^\alpha + \frac{dz^\alpha}{dt} f^t, \quad (64)$$

where

$$a_p^\alpha \equiv \frac{d^2 z^\alpha}{dt^2} + \left(\Gamma^\alpha_{\beta\gamma} - \frac{dz^\alpha}{dt}\Gamma^t_{\beta\gamma}\right)\frac{dz^\beta}{dt}\frac{dz^\gamma}{dt}. \quad (65)$$

The subscript  $p$  refers to the fact that  $a_p^\alpha$  involves only the perturbative terms in  $d^2 z^\alpha/dt^2$ . Indeed, a simple calculation based on the preceding equations for  $d^2 r/dt^2$  and  $d^2 \phi/dt^2$ , as well as the Christoffel symbols obtained from the Schwarzschild metric, reveals that

$$a_p^r = -\frac{M}{r_h^2}\left(\epsilon\tilde{A} + \epsilon\tilde{B}\frac{dr}{dt}\right), \quad (66)$$

$$a_p^\phi = -\frac{M}{r_h^2}\epsilon\tilde{B}\frac{d\phi}{dt}. \quad (67)$$

Equation (64) determines  $f^r$  and  $f^\phi$  in terms of  $f^t$ . The orthogonality condition (39) then allows us to find all three components of the force. The result is

$$f^t = \frac{\dot{t}^2 \left[ a_p^r \frac{dr}{dt} + a_p^\phi r^2 F \frac{d\phi}{dt} \right]}{F^2 - \left( \frac{dr}{dt} \right)^2 - F r^2 \left( \frac{d\phi}{dt} \right)^2}, \quad (68)$$

$$f^r = \frac{\dot{t}^2 \left[ a_p^r \left( F - r^2 \left( \frac{d\phi}{dt} \right)^2 \right) + a_p^\phi r^2 \frac{dr}{dt} \frac{d\phi}{dt} \right]}{F^{-1} \left( F^2 - \left( \frac{dr}{dt} \right)^2 - F r^2 \left( \frac{d\phi}{dt} \right)^2 \right)}, \quad (69)$$

$$f^\phi = \frac{\dot{t}^2 \left[ a_p^r \frac{dr}{dt} \frac{d\phi}{dt} + a_p^\phi \left( F^2 - \left( \frac{dr}{dt} \right)^2 \right) \right]}{F^2 - \left( \frac{dr}{dt} \right)^2 - F r^2 \left( \frac{d\phi}{dt} \right)^2}. \quad (70)$$

Substituting  $a_p^\alpha$  into the above results, and using the normalization condition  $-1 = \dot{z}^\alpha \dot{z}_\alpha = -F \dot{t}^2 + F^{-1} \dot{r}^2 + r^2 \dot{\phi}^2$ , leads to

$$\begin{aligned} f^r &= -\frac{\epsilon M \dot{t}^4}{r_h^2} \left\{ \left[ F - r^2 (d\phi/dt)^2 \right] \tilde{A} + F (dr/dt) \tilde{B} \right\}, \\ f^\phi &= -\frac{\epsilon M \dot{t}^4}{r_h^2} \frac{d\phi}{dt} \left\{ F^{-1} (dr/dt) \tilde{A} + F \tilde{B} \right\}. \end{aligned} \quad (71)$$

Since  $f^t$  is not required in our formalism, we will not provide an explicit expression for it.

We can recast these equations in a form analogous to that of Eqs. (59) and (60),

$$f^r = -\frac{\mu}{r^2} \left[ \mathcal{A} + \mathcal{B} \frac{dr}{dt} \right], \quad (72)$$

$$f^\phi = -\frac{\mu}{r^2} \mathcal{B} \frac{d\phi}{dt}, \quad (73)$$

by defining  $\mathcal{A}$  and  $\mathcal{B}$  as

$$\mathcal{A} = \frac{\dot{t}^2}{(1 - M/r)^2} \tilde{A}, \quad (74)$$

$$\mathcal{B} = \frac{\dot{t}^4}{(1 - M/r)^2} \left( \frac{1}{F} \frac{dr}{dt} \tilde{A} + F \tilde{B} \right). \quad (75)$$

The factors of  $\dot{t}$  convert the “time” variable in the acceleration from coordinate time to proper time; this is given by

$$\dot{t}^2 = \frac{1}{F - F^{-1} (dr/dt)^2 - r^2 (d\phi/dt)^2}, \quad (76)$$

where, we recall,  $F = 1 - 2M/r$ . The factors of  $1/(1 - M/r)^2$ , on the other hand, convert from harmonic coordinates to Schwarzschild coordinates. One could incorporate these factors into each  $\tilde{A}_i$  and  $\tilde{B}_i$  and then re-expand these in powers of  $M/r$  to find new expressions for  $\mathcal{A}_i$  and  $\mathcal{B}_i$ , neglecting terms of 3PN order and higher; but since the hybrid equations already introduce errors above 2.5PN order, doing so is unnecessary. Thus, for simplicity we shall use the force in its above form.

The final expression for the perturbing force is obtained by substituting the post-Newtonian expansions

for  $\tilde{A}$  and  $\tilde{B}$  into Eqs. (74) and (75); the relevant equations are listed near the beginning of Sec. III A. In these equations we must make the substitution  $r_h = r - M$ , and convert  $t$ -derivatives into  $\chi$ -derivatives by employing Eq. (26). In these final forms, the expressions for  $f^r$  and  $f^\phi$  are ready to be inserted within the evolution equations for the orbital elements.

## B. Results

### 1. Adiabatic, secular, and radiative approximations

We are primarily interested in determining the types of errors introduced by the adiabatic and radiative approximations. We should first clarify the meaning of these approximations. The basis of both approximations in the context of osculating orbits is the separation of orbital elements into secular and oscillating parts, i.e.  $I^A = I_{\text{sec}}^A + I_{\text{osc}}^A$ . The particular adiabatic approximation that we are concerned with, which we have titled “secular approximation,” is one which eliminates the oscillations and keeps only the secular behavior; that is, it uses an approximate orbital evolution with  $I_{\text{adb}}^A = I_{\text{sec}}^A$ . A radiative approximation uses only dissipative terms in the perturbing force, with orbital elements  $I_r^A$ , with the hope that the secular part  $I_{\text{sec}}^A$  of this evolution reproduces  $I_{\text{sec}}^A$ .

Unfortunately, these general definitions are somewhat ambiguous. We examine first the case of the secular approximation. The main source of ambiguity associated with the general idea of removing oscillations is that it is not clear *which oscillations* are intended to be removed. For example, in the formalism presented in this paper, removing the oscillations with respect to  $\chi$  will not remove the oscillations with respect to  $t$ , and vice versa. This failure is caused by the zeroth-order (i.e. geodesic) oscillations in time as a function of  $\chi$ . Consequently, a secular evolution defined by an average over the orbital parameter  $\chi$ , such as

$$I_{\text{sec}}^A = \langle I^A \rangle_\chi \equiv \frac{1}{2\pi} \int_{\chi-\pi}^{\chi+\pi} I^A(\chi') d\chi', \quad (77)$$

will differ from that defined by an average over time, such as

$$I_{\text{sec}}^A = \langle I^A \rangle_t \equiv \frac{\int_{\chi-\pi}^{\chi+\pi} I^A \frac{dt}{d\chi} d\chi'}{\int_{\chi-\pi}^{\chi+\pi} \frac{dt}{d\chi} d\chi'}. \quad (78)$$

A precise definition of a secular approximation would have to specify which averaging procedure is to be selected.

A second source of ambiguity concerns the choice of initial conditions. We desire that our secular evolution reproduce the average of the true evolution, and this means that in general, the initial conditions placed on

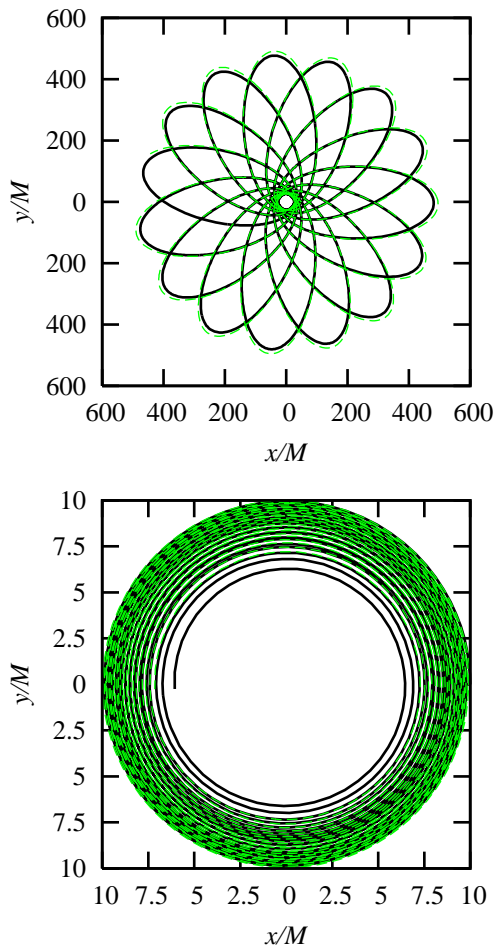


FIG. 1: Comparisons of true orbits (solid black curves) and radiative approximation orbits (dashed green curve) with identical initial conditions and with a mass ratio  $\mu/M = 0.01$ . In each case the two orbits begin at periapsis and are terminated at the same final time. Upper plot: highly eccentric orbits with  $p_0 = 50$  and  $e_0 = 0.9$ . At the end of the simulation the approximate orbit lags behind the true orbit by approximately one-half radial cycle out of a total of fifteen. Lower plot: quasi-circular orbits with identical initial conditions  $p_0 = 10$  and  $e_0 = 0$ . Again, the approximate orbit lags behind the true orbit.

the approximate solution will have to differ from the exact initial conditions. This is because the exact solution contains the secular approximation plus oscillations, and the oscillations may not vanish at the initial time. Identifying the correct initial conditions for the approximate evolution therefore requires knowledge of the oscillations; in the absence of such information—that is, when the exact solution is not known—the initial conditions remain unknown and the procedure is ambiguous. The ambiguity persists even when the exact solution is known, because it is then inherited from the first source of ambiguity, the question as to which oscillations are to be removed. The ambiguity associated with the initial

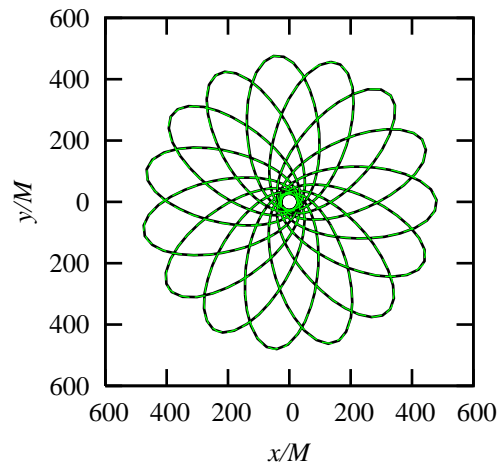


FIG. 2: The same eccentric orbit as shown in Fig. 1, but now using time-averaged initial conditions for the radiative approximation. In this case the approximate orbit is indistinguishable from the true orbit on the timescale of the plot (fifteen orbital cycles).

conditions is lifted only when the averaging procedure is selected, and when the exact solution is known; the approximate initial conditions are then calculated by averaging the exact evolution over the first radial cycle. For example, in the case of an averaging over  $\chi$  we would set  $I_{\text{sec}}^A(0) = (2\pi)^{-1} \int_0^{2\pi} I^A(\chi) d\chi$ .

We shall not pursue a detailed exploration of the ambiguities associated with the secular approximation in this paper, although they are quite important; they are the focus of a companion paper [17]. Our focus here will be instead on the limitations and ambiguities of the radiative approximation. As was indicated previously, a radiative evolution switches off all conservative terms in the perturbing force ( $\tilde{A}_1 = \tilde{A}_2 = \tilde{B}_1 = \tilde{B}_2 = 0$ ), and retains only the radiative terms at 2.5PN order ( $\tilde{A}_{2.5} \neq 0$  and  $\tilde{B}_{2.5} \neq 0$ ). This approximation is logically distinct from adiabatic approximations in general, but the hope formulated in the literature (for example in Refs. [18, 19, 20]) is that the radiative evolution will reproduce the secular changes of the orbital elements. We shall see that while the radiative approximation captures the secular changes in  $p(\chi)$  and  $e(\chi)$ , it fails to account for secular changes in  $w(\chi)$ ,  $t(\chi)$ , and  $\phi(\chi)$ ; this conclusion confirms and extends those of our previous work [16, 17].

In addition, the radiative approximation is subject to the same ambiguities regarding the choice of initial conditions as the secular approximation. Writing the radiative evolution as the sum of its secular and oscillatory parts,  $I_r^A(\chi) = I_r^A{}_{\text{sec}} + I_r^A{}_{\text{osc}}$ , we shall consider three possible candidates for  $I_r^A(0)$ . The first is  $I_r^A(0) = I^A(0)$ , the exact initial data that is selected for the true evolution of the orbital elements under the action of the full perturbing force. The second is  $I_r^A{}_{\text{sec}} = \langle I^A \rangle_\chi(0)$ , the  $\chi$ -averaged initial data, which identifies the initial

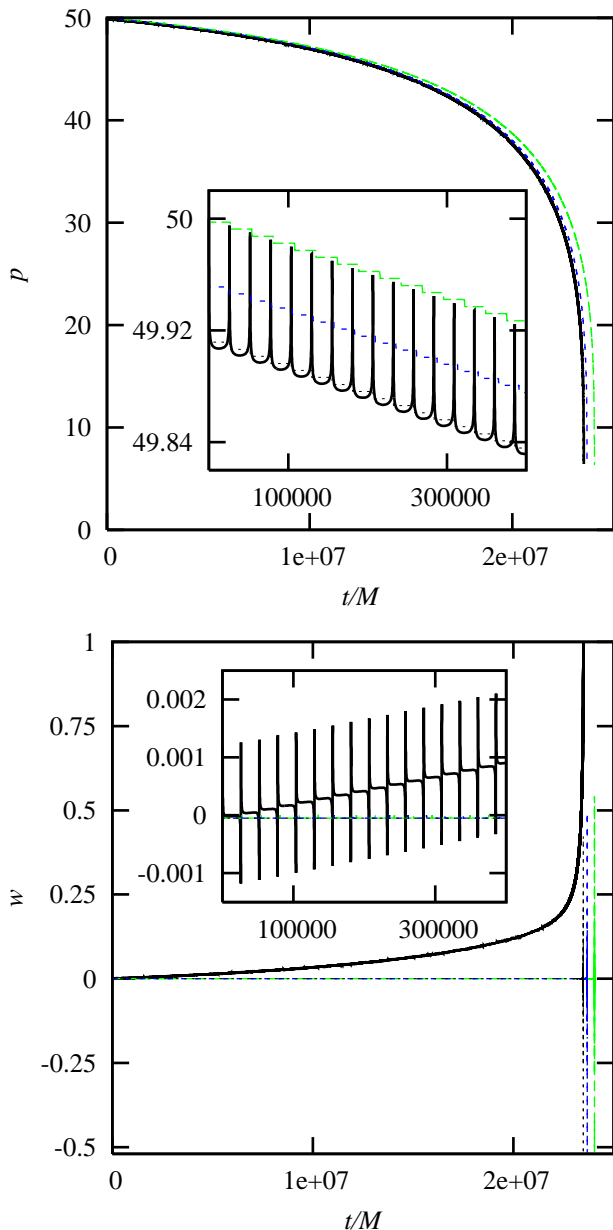


FIG. 3: The principal element  $p$  and positional element  $w$  as functions of time for a complete inspiral, beginning with the initial conditions of the eccentric orbit in Fig. 1. In each plot the true curve is in solid black, the radiative curve with the same initial conditions is long-dashed in green (the uppermost curve in the  $p$  plot), the radiative curve with  $\chi$ -averaged initial conditions is short-dashed in blue (middle curve in  $p$  plot), and the radiative curve with time-averaged initial conditions is dotted in black (lowest curve in  $p$  plot). The insets display the early behavior of the curves, covering the same range of time as in Fig. 1.

secular part of the radiative evolution with the initial  $\chi$ -averaged part of the true evolution. The third choice is  $I_{r\text{sec}}^A(0) = \langle I^A \rangle_t(0)$ , the  $t$ -averaged initial data, which

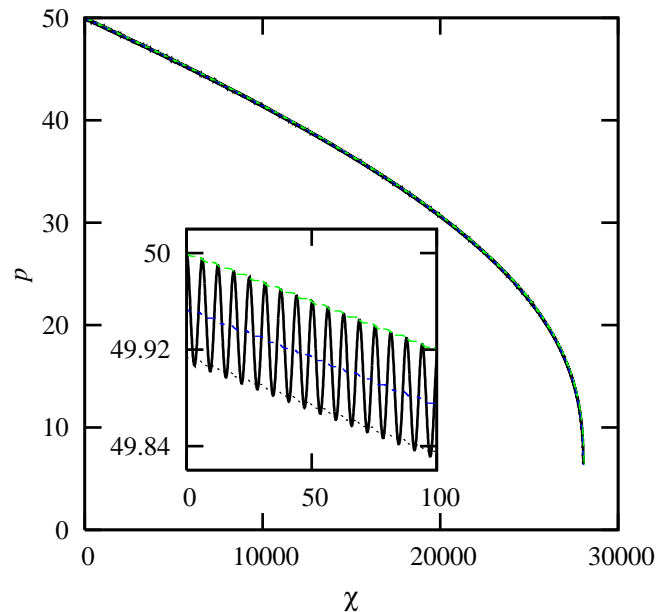


FIG. 4: The principal element  $p$  as a function of the orbital parameter  $\chi$ . The curves are as described in Fig. 3. The radiative curves do deviate secularly from the true curve, but the errors are too small to appear on the scale of the graph.

identifies the initial secular part of the radiative evolution with the initial  $t$ -averaged part of the true evolution. (We note that for both the second and third choices of initial conditions, the initial value  $I_r^A(0)$  is not fixed by  $I_{r\text{sec}}^A(0)$  alone, since we also require the initial value of  $I_{r\text{osc}}^A$ . Although we do not have *a priori* access to this oscillatory part, we can assign it an approximate initial value based on the results of the radiative evolution with exact initial conditions. This introduces a negligible error, since the oscillations in the radiative evolution are extremely small in practice.) These three choices of initial data are distinct, and they lead to different evolutions. We shall see that the accuracy of the evolution (relative to the true evolution) depends strongly on the choice of initial data.

## 2. Orbital evolution

A typical inspiral of interest for LISA will form in a highly eccentric state. Over the course of the inspiral the system will emit gravitational radiation carrying away energy and angular momentum, shrinking and circularizing the orbit over time. Thus, the inspiral will evolve from a highly eccentric orbit to a quasi-circular one, and it will end in a rapid plunge. We shall now determine the validity of the radiative approximation for this class of orbits. Since our perturbing force is valid only in the post-Newtonian regime, we always ensure that  $v^2 \lesssim 0.1$ .

The general limitations of the radiative approximation are demonstrated in Fig. 1, which displays the spa-

tial trajectories of a highly eccentric orbit and a quasi-circular orbit, along with corresponding radiative approximations. In each case the true and approximate orbits are terminated at identical final times, at which point the radiative approximation lags behind the true orbit. With a mass ratio of  $\mu/M = 0.01$ , this dephasing of the two orbits is noticeable after only fifteen radial cycles in the eccentric case, while several dozen revolutions are required in the quasi-circular case. Since the dephasing is apparent before any non-geodesic precession occurs, we interpret its cause to be conservative effects in the time-dependence of the orbit. That is, the error in  $t(\chi)$  dominates over the errors in  $w(\chi)$  and  $\phi(\chi)$ , such that the particle lies at the wrong spatial point at a given time, even before  $r(\chi)$  and  $\phi(\chi)$  have deviated significantly from the true orbit.

For the plots in Fig. 1 we have chosen exact initial conditions  $I^A(0)$  for the approximate orbit. By choosing averaged initial conditions we obtain better results in the eccentric case: as shown in Fig. 2, using time-averaged initial conditions  $\langle I^A \rangle_t(0)$  eliminates the dephasing on the timescale of the plot. Using  $\chi$ -averaged initial conditions  $\langle I^A \rangle_\chi(0)$  results in a smaller improvement, as we will discuss below. However, in the quasi-circular case all initial conditions fare equally well.

The evolution of the orbital elements over a complete inspiral, beginning with the initial conditions of the eccentric orbit in Fig. 1 and continuing to quasi-circularity, is displayed in Fig. 3. Insets in the plots display the same range of time covered by Fig. 1. The orbit stops before the final plunge of the small body into the large black hole. There are two reasons for this truncation. First, our method of osculating orbits cannot cover the final plunge, because of the underlying restriction that the orbit must be bounded between a minimum radius  $pM/(1+e)$  and a maximum radius  $pM/(1-e)$ ; this is reflected mathematically by the condition  $p > 6 + 2e$ , which is violated during plunge. Second, we should in any case leave this portion of the orbit alone, because the velocities and fields therein are highly relativistic; in this regime the post-Newtonian expansion of the perturbing force becomes inaccurate. In Fig. 3 we display results of the numerical evolution for the principal element  $p$  and positional element  $w$  only; the evolution of  $e$  is qualitatively similar to that of  $p$ . It is worth noting, however, that the eccentricity never quite reaches  $e \approx 0$ ; instead, quasi-circularity is manifested by the condition  $\chi - w \approx 0$ , which equally well ensures that  $r' \approx 0$ . This observation agrees with the results of Ref. [24].

The results for all three choices of initial conditions are plotted in Fig. 3. As we see from these plots, the radiative approximation qualitatively matches the true secular evolution for the principal element  $p$ , but neglects all secular changes in the positional element  $w$ . This is the expected result. However, we also see that the radiative approximation deviates from the true evolution even for the principal element. The extent of this deviation depends on the choice of initial conditions, with the

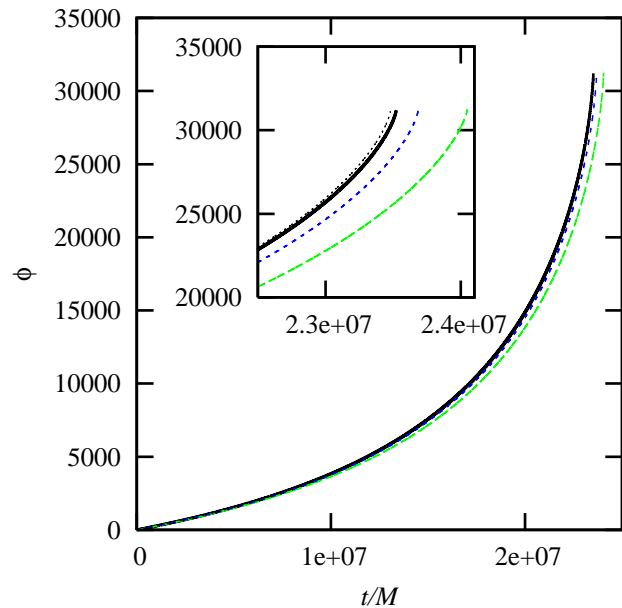


FIG. 5: The orbital phase  $\phi$ , with curves as described in Fig. 3. The scale of the plot suggests that the radiative evolution with time-averaged initial data (the uppermost curve in dotted black) gives an accurate approximation of the true evolution. The vertical scale, however, is large, and this is a false impression. At the late time  $t/M = 2.345 \times 10^7$ , the error in phase is  $\Delta\phi = 4520$  rad for the exact initial data,  $\Delta\phi = 1830$  rad for the  $\chi$ -averaged initial data, and  $\Delta\phi = 655$  rad for the  $t$ -averaged initial data. This last choice fares best, but its accuracy is poor over a complete inspiral.

time-averaged initial conditions faring the best and exact initial conditions the worst.

An essential aspect of our results is that the errors in the principal elements produced by the radiative approximation are mostly due to errors in  $t(\chi)$ . As we see in Fig. 4, the errors almost completely vanish when the principal elements are plotted as functions of  $\chi$ ; significant errors arise only in the conversion between  $\chi$  and  $t$ .

### 3. Errors in orbital phase

The errors in which we are most interested are errors in orbital phase, since they will lead directly to errors in the phase of the emitted gravitational radiation. Figure 5 displays the phase  $\phi$  versus time, again using all three choices of initial conditions for the radiative approximation. Once again we see that the time-averaged conditions produce the smallest error, for the same reasons described in the previous section.

Figure 6 shows the dependence of the dephasing  $\Delta\phi = \phi - \phi_{\text{rad}}$  on the parameters of the problem. We plot the dephasing for a “radiation-reaction” time defined by  $p \rightarrow 0.9p_0$ , rather than a complete inspiral, since

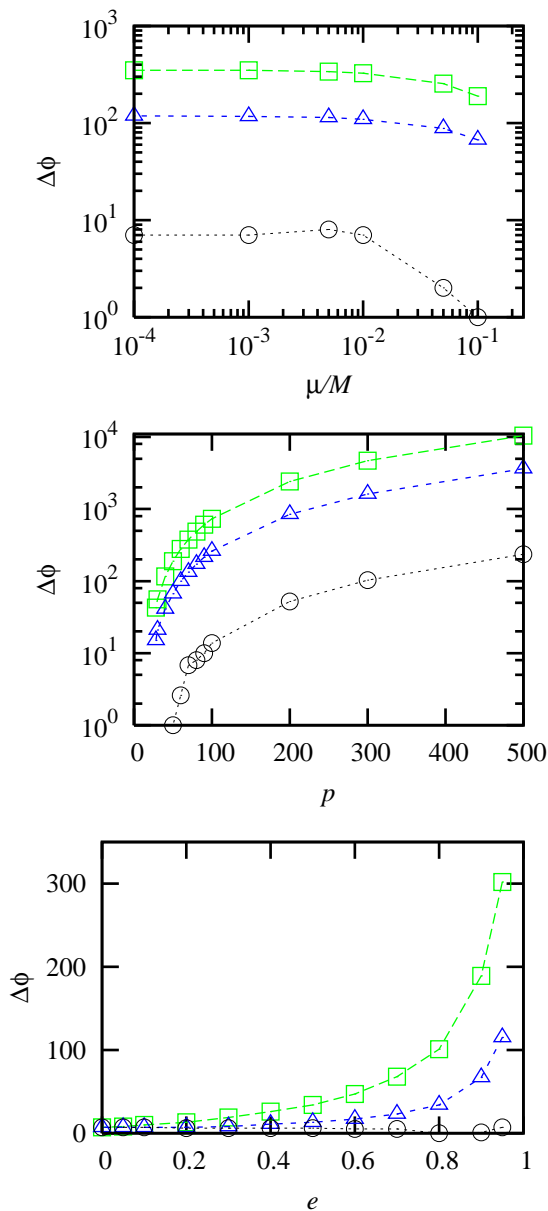


FIG. 6: The difference in orbital phase  $\phi$  between the true orbit and approximate orbits after a radiation-reaction time (defined by  $p \rightarrow 0.9p_0$  on the true orbit). Open squares indicate results for identical initial conditions, open triangles for matching  $\chi$ -averaged initial conditions, and open circles for matching  $t$ -averaged initial conditions. Top: dephasing as a function of the mass ratio  $\mu/M$ , with fixed true initial values  $p_0 = 50$  and  $e_0 = 0.9$ . The dephasing becomes  $\mu$ -independent for sufficiently small  $\mu$ , when second-order effects become negligible. Middle: dephasing as a function of initial value  $p_0$ , with fixed  $e_0 = 0.9$  and  $\mu/M = 0.1$ . Bottom: dephasing as a function of initial eccentricity  $e_0$ , with fixed  $p_0 = 50$  and  $\mu/M = 0.1$ . The error in the case of time-averaged initial conditions is approximately independent of  $e$ .

gravitational-wave data analysis may require only a portion of a complete inspiral. We see that the dephasing is

independent of  $\mu$  for sufficiently small values of  $\mu$ . This is an expected result, since the radiation-reaction time at leading order in  $\mu$  varies as  $1/\mu$ , while the rate of dephasing varies as  $\mu$ , leading to a net cancellation in the total dephasing. However, terms in the perturbing force that are quadratic in  $\mu$  alter this result when  $\mu/M$  is sufficiently large. Somewhat surprisingly, these quadratic terms actually serve to decrease the dephasing, lowering the impact of conservative terms in the force.

As expected, the dephasing decreases at lower values of  $e$ , although the eccentricity seems to have negligible impact in the case of time-averaged initial conditions. Also as expected, the dephasing varies as  $p^{3/2}$ , regardless of initial conditions. This scaling follows from the form of the post-Newtonian force: the leading-order conservative term enters at 1PN order, which scales as a  $p^{-1}$  correction to Newtonian gravitation, while the leading-order dissipative term enters at 2.5PN order, which scales as a  $p^{-5/2}$  correction. The dephasing is governed by the relative strength of the conservative terms, leading to a scaling of  $p^{-1}/p^{-5/2} = p^{3/2}$ .

In all cases the time-averaged initial conditions yield the best results. Indeed, the efficacy of these initial conditions is almost surprising. One way of understanding their impact is to examine the insets in Fig. 3. Peaks in the true curve correspond to the short periods of time near periapsis, while relatively flat regions correspond to the long periods of time around apoapsis. Thus, choosing exact initial conditions matches the true and approximate orbits for the minimal amount of time, as well as in the region of strongest fields, leading to the largest possible deviation. Choosing time-averaged initial conditions matches the orbits near apoapsis, for the longest time and with the weakest fields, leading to the least possible deviation. The  $\chi$ -averaged initial conditions are then in some sense the average of all the incorrect choices. An implication of this is that in some circumstances the  $\chi$ -averaged initial conditions could turn out to be even worse than the exact initial conditions. For example, choosing exact initial conditions at apoapsis would closely approximate the time-averaged initial conditions, which would then fare much better than the  $\chi$ -averaged initial conditions.

We can explain the long-term impact of the initial conditions by considering the time-dependence of an orbit. The secular time function  $\langle t \rangle(\chi)$  can be written in terms of the orbital period  $P(\chi) = \int_{\chi-\pi}^{\chi+\pi} t'(\tilde{\chi}) d\tilde{\chi}$  as  $\langle t \rangle(\chi) = \int_0^\chi P(\tilde{\chi}) d\tilde{\chi}$ . As we see from the insets in Fig. 3, the changes in initial conditions bring the initial orbital period of the radiative approximation closer to that of the true orbit; and as we would intuitively expect, the time-averaged initial conditions best reproduce the initial temporal period. This correction,  $\delta P$ , to the initial period then induces a long-term correction to  $\langle t \rangle(\chi)$  of the form  $\delta \langle t \rangle \sim \chi \cdot \delta P$ . (Such an effect can be calculated explicitly for the electromagnetic self-force considered in Ref. [17]: refer to Eqs. (4.8) and (4.21) therein.) In essence, the time-averaged initial conditions carry information about the initial conservative correction to the true orbital pe-

riod, and they thus implicitly insert a conservative correction into the radiative approximation. This serves to remind us that we would have difficulty choosing suitable initial conditions for the radiative approximation if we did not have prior access to the true evolution.

Regardless of the choice of initial conditions, one should note that the errors accumulated over a complete inspiral are much larger than those shown in Fig. 6. (Refer to the caption of Fig. 5 for actual values.) Also, the plots of  $\Delta\phi$  versus  $p$  and  $e$  are for  $\epsilon = 0.1$ , leading to a smaller dephasing than would occur if  $\epsilon$  were in the region of linear dominance. Thus, even if ideal initial conditions could be found without reference to the exact solution, the radiative approximation would generically fail over a complete inspiral.

#### 4. Gauge dependence

As is well known, the gravitational self-force is a gauge-dependent quantity: it is not invariant under a change of coordinates  $x^\mu \rightarrow x^\mu + \xi^\mu$ , where  $\xi^\mu$  is a “small” vector field. The equations of motion that we have used in this paper were calculated within the harmonic gauge of post-Newtonian theory, and the magnitudes of the conservative effects that we have displayed refer to this particular gauge choice; different gauges would necessarily lead to different results. Indeed, Mino has argued in favor of constructing a physically meaningful “radiation-reaction gauge” in which the conservative effects of the self-force are set to zero over a finite radiation-reaction time, making the radiative approximation exact over that interval [13, 25]. Mino has also argued that this gauge choice induces a change in initial conditions that partially absorbs conservative effects [13], and this statement agrees with our result that long-term conservative effects can be mimicked by a small change in initial conditions. We would like to point out, however, that a rigorous construction and implementation of such a gauge choice have yet to be performed, and that the impact of making this choice on quantities other than the self-force has yet to be determined.

It is known, for example, that in the harmonic gauge of post-Newtonian theory, the equations of motion contain both radiative and conservative terms, and that the gravitational potentials are well-behaved everywhere, except at the position of each (pointlike) body where they diverge with an expected power of  $m/r$ . What is the behavior of the gravitational potentials in Mino’s radiation-reaction gauge? The answer is not known, and it would be interesting to investigate the issue in post-Newtonian theory. For example, one could determine the effect on the potentials of making a coordinate transformation that would turn off some of the conservative terms in the equations of motion (those that depend on  $\epsilon$  in Sec. IIIA); would this spoil the behavior of the potentials near the bodies, or perhaps elsewhere in the spacetime? Such an analysis would be revealing, and it would give indication

as to whether Mino’s scheme is likely to be successfully implemented.

We believe that the Lorenz gauge of the gravitational self-force problem, which is in close mathematical analogy with the harmonic gauge of post-Newtonian theory, is also in close physical analogy: it produces conservative terms in the self-force, and it produces gravitational potentials that are well behaved everywhere (except at the position of the orbiting body). Given the successes of post-Newtonian theory in its harmonic-gauge formulation, we feel confident that the Lorenz gauge is ultimately a better choice of gauge for the gravitational self-force problem, in spite of the presence of conservative terms in the equations of motion. We shall therefore defer our judgment on the advantages of Mino’s radiation-reaction gauge, and reiterate the importance of the conservative terms in the harmonic-gauge (or Lorenz-gauge) self-force. Our conclusions, to be sure, apply within the confines of the post-Newtonian harmonic gauge. But we contend that our conclusions are in fact generic: Outside of a finely-tuned gauge choice, one should expect the conservative part of the self-force to produce large secular effects.

## IV. CONCLUSION

The first part of this paper was devoted to the development of a method of osculating orbits to integrate the equations of motion that govern bound, accelerated orbits in Schwarzschild spacetime. The method involves the phase-space variables  $\{p, e, w, t, \phi\}$ , which are expressed as functions of an orbital parameter  $\chi$ ; each variable satisfies a first-order differential equation, and knowledge of these variables is sufficient to determine the worldline in spacetime. Although the method is limited to situations in which the force acts within the orbital plane, this limitation can be overcome; in addition, the force is not assumed to be small. We show in Appendix A that for large values of  $p$ , our equations reduce to the standard perturbation equations of Newtonian celestial mechanics. The method has many potential applications, including the important one of permitting an implementation of the gravitational self-force. Most immediately, it provides an attractive conceptual and mathematical foundation for a perturbative approach to weakly accelerated orbits. And furthermore, the method is easy to implement in practice in a numerical code.

In the second part of the paper we applied the method of osculating orbits to the inspiral of a small body into a Schwarzschild black hole of much larger mass. The perturbing force was calculated on the basis of the hybrid Schwarzschild/post-Newtonian equations of motion of Kidder, Will, and Wiseman [14], and its effect on the orbiting body was obtained by numerical integration of our evolution equations for the dynamical variables  $\{p, e, w, t, \phi\}$ . This approach is well suited to a study of the limitations and ambiguities of adiabatic and radiative

approximations, which was carried out next. Specifically, we have illustrated the importance of conservative effects in the time dependence of the orbit, and we have established the advantage of choosing time-averaged initial conditions for the approximated orbital elements. This problem differs in many respects from the fully relativistic self-force problem, but it nevertheless captures many of its essential features. Our conclusions, therefore, might be expected to hold in the fully relativistic case for most choices of gauge.

### Acknowledgments

We wish to thank the referee for several helpful suggestions. This work was supported by the Natural Sciences and Engineering Research Council of Canada.

### APPENDIX A: NEWTONIAN LIMIT

Since our work extends the standard methods of Newtonian celestial mechanics, it is a worthwhile endeavor to show that our equations reduce to those for perturbed Keplerian orbits in Newtonian mechanics. In this Appendix we derive the Newtonian limit of our expressions by expanding in powers  $p^{-1}$ ; since  $p^{-1} \propto r^{-1} \sim v^2$ , this is equivalent to a post-Newtonian expansion. We shall first describe the general relationship between the Newtonian and relativistic perturbing forces. Next we shall show that our geodesic parametrization reduces to Keplerian ellipses and that our evolution equations for the orbital elements  $p$ ,  $e$ , and  $w$  reduce to Gauss' perturbation equations of celestial mechanics.

Substituting the Christoffel symbols of the Schwarzschild metric into the equations of motion (2) yields the following equations for the force:

$$f^r = \ddot{r} + F \frac{M}{r^2} \dot{t}^2 - F^{-1} \frac{M}{r^2} \dot{r}^2 + F \dot{\phi}^2, \quad (\text{A1})$$

$$f^\phi = \ddot{\phi} + 2 \frac{\dot{r} \dot{\phi}}{r}, \quad (\text{A2})$$

$$f^t = \ddot{t} + F^{-1} \frac{2M}{r^2} \dot{r}^2, \quad (\text{A3})$$

where  $F = 1 - 2M/r$ . The time-component of the force can be written in a more useful form using the orthogonality relation (39).

These expressions for the relativistic force differ non-trivially from those in the Newtonian case. We define  $\tilde{F}$ , the Newtonian perturbing force per unit mass, via Newton's second law:

$$\ddot{\mathbf{x}} = \mathbf{g} + \tilde{F}, \quad (\text{A4})$$

where  $\mathbf{x}$  is a 3-vector representing the spatial coordinates of the particle and  $\mathbf{g} = -\frac{M}{r^2} \hat{\mathbf{r}}$  is the Newtonian gravitational acceleration. For convenience we have defined the Newtonian acceleration as the second derivative of  $\mathbf{x}$  with

respect to proper time rather than coordinate time. We also define the radial and tangential components of the perturbing force via

$$\tilde{F} \equiv \tilde{F}^r \hat{\mathbf{r}} + \tilde{F}^\phi \hat{\boldsymbol{\phi}}, \quad (\text{A5})$$

where  $\hat{\mathbf{r}}$  and  $\hat{\boldsymbol{\phi}}$  form an orthonormal basis in the orbital plane. Given these definitions, writing  $\ddot{\mathbf{x}}$  in polar coordinates  $(r, \phi)$  leads to

$$\tilde{F}^r = \ddot{r} - r \dot{\phi}^2 + \frac{M}{r^2} \quad (\text{A6})$$

$$\tilde{F}^\phi = r \ddot{\phi} + 2 \dot{r} \dot{\phi}. \quad (\text{A7})$$

Comparing the Newtonian and relativistic expressions for the perturbing force, we see they are related by the equations

$$f^r = \tilde{F}^r + r(1-F) \dot{\phi}^2 + \frac{M}{r^2} (F \dot{t}^2 + F^{-1} \dot{r}^2 - 1), \quad (\text{A8})$$

$$f^\phi = \frac{\tilde{F}^\phi}{r}. \quad (\text{A9})$$

Thus,  $f^r$  differs from  $\tilde{F}^r$  by relativistic corrections, while  $f^\phi$  differs from  $\tilde{F}^\phi$  only by a factor of the orbital radius.

We next consider our parametrization of geodesics. From Eqs. (24), (26), and (21) one trivially finds the leading-order terms in  $\phi'$ ,  $t'$ , and  $\dot{\chi}$  to be

$$\phi' = 1, \quad (\text{A10})$$

$$t' = \frac{p^{3/2} M}{[1 + e \cos(\chi - w)]^2}, \quad (\text{A11})$$

$$\dot{\chi} = \frac{[1 + e \cos(\chi - w)]^2}{p^{3/2} M}. \quad (\text{A12})$$

Thus, in the Newtonian limit we have  $\phi = \chi$  and  $t = \tau$  and the resulting parametrization

$$r = \frac{pM}{1 + e \cos(\phi - w)}, \quad (\text{A13})$$

$$\frac{d\phi}{dt} = \frac{[1 + e \cos(\phi - w)]^2}{p^{3/2} M}. \quad (\text{A14})$$

In terms of the orbital elements, we see that  $w = \Phi$  in the Newtonian limit. This corresponds to the loss of one degree of freedom, as we would expect from the fact that  $t$  in Newtonian physics is a universal parameter rather than a coordinate. We can also easily find that the energy and angular momentum per unit mass reduce to  $E = 1 - \frac{1-e^2}{2p}$  and  $L = \sqrt{p}M$ , respectively. The first term in  $E$  is the rest energy of the particle, while the second term is the Newtonian energy  $\frac{1}{2}v^2 - \frac{M}{r}$ .

With the exception of the inclusion of the rest mass, the above results are standard Keplerian relationships. Thus, our equations for the orbital elements should reduce to those for perturbed Keplerian orbits. Substituting Eqs. (A10)–(A12) into Eqs. (39), (A8), and (A9),



we find the leading-order expressions for the perturbing force:

$$f^r = \tilde{F}^r \quad (\text{A15})$$

$$f^\phi = \frac{\tilde{F}^\phi}{r} \quad (\text{A16})$$

$$f^t = \frac{e \sin(\phi - w)}{\sqrt{p}} \tilde{F}^r + \frac{1 + e \cos(\phi - w)}{\sqrt{p}} \tilde{F}^\phi. \quad (\text{A17})$$

These results allow us to expand Eqs. (36), (37), and (38) to find the leading-order expressions for the orbital elements:

$$\frac{dp}{dt} = \frac{2p^{3/2}}{1 + e \cos(\phi - w)} \tilde{F}^\phi \quad (\text{A18})$$

$$\begin{aligned} \frac{de}{dt} &= \sqrt{p} \frac{e + 2 \cos(\phi - w) + e \cos^2(\phi - w)}{1 + e \cos(\phi - w)} \tilde{F}^\phi \\ &+ \sqrt{p} \sin(\phi - w) \tilde{F}^r \quad (\text{A19}) \end{aligned}$$

$$\begin{aligned} \frac{dw}{dt} &= \frac{\sqrt{p} M^{3/2}}{e} \frac{\sin(\phi - w)[2 + e \cos(\phi - w)]}{1 + e \cos(\phi - w)} \tilde{F}^\phi \\ &- \frac{\sqrt{p} M^{3/2}}{e} \cos(\phi - w) \tilde{F}^r. \quad (\text{A20}) \end{aligned}$$

These are Gauss' well known perturbation equations.

## APPENDIX B: EVOLUTION EQUATIONS FROM KILLING VECTORS

It is possible to derive Eqs. (36)–(38) for the derivatives of the osculating elements from Eq. (10) and the Killing vectors of the Schwarzschild spacetime, without reference to Eq. (11). Although this derivation is equivalent to that given in Sec. II C, its physical significance is more intuitive. We begin by defining energy and angular momentum (per unit mass) as  $E = -\xi_{(t)}^\alpha \dot{z}_\alpha$  and

$L = \xi_{(\phi)}^\alpha \dot{z}_\alpha$ , where  $\xi_{(t)} = \frac{\partial}{\partial t}$  and  $\xi_{(\phi)} = \frac{\partial}{\partial \phi}$  are Killing vectors corresponding to the spacetime's invariance under time translations and spatial rotations. From these definitions we find

$$\begin{aligned} -\dot{E} &= \dot{z}^\beta (\xi_{(t)}^\alpha \dot{z}_\alpha)_{;\beta} \\ &= \xi_{(t); \beta}^\alpha \dot{z}_\alpha \dot{z}^\beta + \xi_{(t)}^\alpha \dot{z}^\beta \dot{z}_{\alpha; \beta} \\ &= \xi_{(t)}^\alpha f_\alpha. \quad (\text{B1}) \end{aligned}$$

The first term on the second line vanishes due to the antisymmetry of  $\xi_{\alpha; \beta}$  for any Killing vector  $\xi$ , and the final line then follows from the equation of motion  $\dot{z}^\alpha \dot{z}^\beta_{;\alpha} = f^\beta$ . An analogous result holds for  $\dot{L}$ . From the definitions of  $\xi_{(t)}$  and  $\xi_{(\phi)}$  we then find

$$\dot{E} = F f^t, \quad (\text{B2})$$

$$\dot{L} = r^2 f^\phi. \quad (\text{B3})$$

These results can be used to find  $\dot{e}$  and  $\dot{p}$  using Eqs. (17) and (18), which define  $E(p, e)$  and  $L(p, e)$ . Using these relationships, we write  $\dot{E} = \frac{\partial E}{\partial p} \dot{p} + \frac{\partial E}{\partial e} \dot{e}$  and  $\dot{L} = \frac{\partial L}{\partial p} \dot{p} + \frac{\partial L}{\partial e} \dot{e}$ , which can be rearranged to find

$$\dot{p} = \frac{\frac{\partial E}{\partial e} \dot{L} - \frac{\partial L}{\partial e} \dot{E}}{\frac{\partial L}{\partial p} \frac{\partial E}{\partial e} - \frac{\partial L}{\partial e} \frac{\partial E}{\partial p}}, \quad (\text{B4})$$

$$\dot{e} = \frac{\frac{\partial L}{\partial p} \dot{E} - \frac{\partial E}{\partial p} \dot{L}}{\frac{\partial L}{\partial p} \frac{\partial E}{\partial e} - \frac{\partial L}{\partial e} \frac{\partial E}{\partial p}}. \quad (\text{B5})$$

The equation for  $\dot{w}$  can then be found from Eq. (10), which leads to Eq. (33), or

$$\dot{w} = \frac{1}{r'} \left( \frac{\partial r}{\partial e} \dot{e} + \frac{\partial r}{\partial p} \dot{p} \right). \quad (\text{B6})$$

The explicit results of these calculations are

$$\begin{aligned} \dot{p} &= -\frac{2p^{1/2}(p-2-2e \cos v)(p-2-2e)^{1/2}(p-2+2e)^{1/2}(p-3-e^2)^{1/2}}{(p-6+2e)(p-6-2e)} f^t \\ &+ \frac{2p^2 M(p-4)^4(p-3-e^2)^{1/2}}{(p-6+2e)(p-6-2e)(1+e \cos v)^2} f^\phi, \quad (\text{B7}) \end{aligned}$$

$$\begin{aligned} \dot{e} &= \frac{(p-6-2e^2)(p-2-2e \cos v)(p-2-2e)^{1/2}(p-2+2e)^{1/2}(p-3-e^2)^{1/2}}{p^{1/2}e(p-6+2e)(p-6-2e)} f^t \\ &- \frac{pM(1-e^2)(p^2-8p+12+4e^2)(p-3-e^2)^{1/2}}{e(p-6+2e)(p-6-2e)(1+e \cos v)^2} f^\phi, \quad (\text{B8}) \end{aligned}$$

$$\begin{aligned} \dot{w} &= -\frac{(2e+(p-6) \cos v)(p-2-2e \cos v)(p-2-2e)^{1/2}(p-2+2e)^{1/2}(p-3-e^2)^{1/2}}{p^{1/2}e^2 \sin v(p-6+2e)(p-6-2e)} f^t \\ &+ \frac{pM\{2e(p^2-8p+32)+[(p^2-8p)(1+e^2)+4e^2(6-e^4)] \cos v\}(p-3-e^2)^{1/2}}{e^2 \sin v(p-6+2e)(p-6-2e)(1+e \cos v)^2} f^\phi. \quad (\text{B9}) \end{aligned}$$

When accompanied by the auxiliary equation (21) for  $\frac{dx}{dt}$ , these equations form a closed, autonomous system for the orbital elements.

The results in this section are equivalent to those in Sec. II C, which can be easily shown by using Eq. (39) to replace  $f^t$  with  $f^r$ . But they are numerically ill-behaved. Specifically,  $\dot{e}$  appears to diverge in the limit

$e \rightarrow 0$ , and  $\dot{w}$  appears to diverge when  $\sin v = 0$  (i.e., at every turning point in the orbit). Although these divergences are canceled analytically by the numerators in each case, they are serious obstacles in a numerical integration. Thus, the equations given in Sec. II C are more practical, though slightly lengthier.

- 
- [1] T. Damour, *300 Years of Gravitation* (Cambridge University Press, Cambridge, England, 1987), pp. 128–198.
- [2] T. Futamase and Y. Itoh, *Living Rev. Rel.* **10** (2007), [Online article]: cited on May 28, 2018, <http://www.livingreviews.org/lrr-2007-2>.
- [3] L. Blanchet, *Living Rev. Relativity* **9** (2006), [Online article]: <http://www.livingreviews.org/lrr-2006-4>.
- [4] The LISA website is located at <http://lisa.jpl.nasa.gov>.
- [5] Y. Mino, M. Sasaki, and T. Tanaka, *Phys. Rev. D* **55**, 3457 (1997), arXiv:gr-qc/9606018.
- [6] T. C. Quinn and R. M. Wald, *Phys. Rev. D* **56**, 3381 (1997), arXiv:gr-qc/9610053.
- [7] E. Poisson, *Living Rev. Rel.* **7** (2004), [Online article]: cited on May 28, 2018, <http://www.livingreviews.org/lrr-2004-6>.
- [8] S. Drasco, *Class. Quant. Grav.* **23**, S769 (2006), gr-qc/0604115.
- [9] L. Taff, *Celestial Mechanics: A Computational Guide for the Practitioner* (John Wiley & Sons, New York, 1985).
- [10] G. Beutler, *Methods of Celestial Mechanics* (Springer, New York, 2005).
- [11] T. Damour and N. Deruelle, *Ann. Inst. Henri Poincaré* **43**, 107 (1985).
- [12] T. Damour, A. Gopakumar, and B. R. Iyer, *Phys. Rev. D* **70**, 064028 (2004), arXiv:gr-qc/0404128.
- [13] Y. Mino, *Prog. Theor. Phys.* **113**, 733-761 (2005), gr-qc/0506003.
- [14] L. E. Kidder, C. M. Will, and A. G. Wiseman, *Phys. Rev. D* **47**, 3281 (1993).
- [15] S. Detweiler and E. Poisson, *Phys. Rev.* **D69**, 084019 (2004), gr-qc/0312010.
- [16] A. Pound, E. Poisson, and B. G. Nickel, *Phys. Rev. D* **72**, 124001 (2005), gr-qc/0509122.
- [17] A. Pound and E. Poisson (2007), in preparation.
- [18] Y. Mino, *Phys. Rev. D* **67**, 084027 (2003), gr-qc/0302075.
- [19] K. Ganz, W. Hikida, H. Nakano, N. Sago, and T. Tanaka (2007), to be published in *Prog. Theor. Phys.*, gr-qc/0702054.
- [20] P. A. Sundararajan, G. Khanna, and S. A. Hughes (2007), preprint, gr-qc/0703028.
- [21] A. Pound, Master's thesis, University of Guelph (2006).
- [22] S. Chandrasekhar, *The Mathematical Theory of Black Holes* (Oxford University Press, New York, 1983).
- [23] C. Cutler, D. Kennefick, and E. Poisson, *Phys. Rev. D* **50**, 3816 (1994).
- [24] C. W. Lincoln and C. M. Will, *Phys. Rev. D* **42**, 1123 (1990).
- [25] Y. Mino, *Prog. Theor. Phys.* **115**, 43-61 (2006), gr-qc/0601019.